



FULL LENGTH ARTICLE

Identification of rare *PTCH1* nonsense variant causing orofacial cleft in a Chinese family and an up-to-date genotype-phenotype analysis

Wenjie Zhong^{a,1}, Huaxiang Zhao^{a,1,2}, Wenbin Huang^a,
Mengqi Zhang^a, Qian Zhang^b, Yue Zhang^c, Chong Chen^c,
Zulihumaer Nueraihemaiti^d, Dilifeire Tuerhong^d,
Huizhe Huang^e, Gulibaha Maimaitili^{c,**}, Feng Chen^{b,*},
Jiuxiang Lin^{a,***}

^a Department of Orthodontics, Peking University School and Hospital of Stomatology, Beijing, 100081, PR China

^b Central Laboratory, Peking University School and Hospital of Stomatology, Beijing, 100081, PR China

^c Department of Stomatology, The Fifth Affiliated Hospital of Xinjiang Medical University, Urumqi, 830000, PR China

^d Xinjiang Medical University, Urumqi, 830000, PR China

^e Chongqing Medical University, Chongqing, 400016, PR China

Received 26 October 2019; received in revised form 10 December 2019; accepted 31 December 2019
Available online 8 January 2020

KEYWORDS

Cleft lip with or without palate;
Clinical genetics;
Genotype-phenotype

Abstract The Patched 1 (*PTCH1*) gene encodes a membrane receptor involved in the Hedgehog (Hh) signaling pathway, an abnormal state of which may result in congenital defects or human tumors. In this study, we conducted whole-exome sequencing on a three-generation Chinese family characterized with variable penetrance of orofacial clefts. A rare heterozygous variant in the *PTCH1* gene (c.2833C > T p.R945X) was identified as a disease-associated

* Corresponding author. Central Laboratory, Peking University School and Hospital of Stomatology, 22 Zhongguancun South Avenue, Haidian District, Beijing, China. Fax: +86 010 82195773.

** Corresponding author. Fax: +86 0991 75556479.

*** Corresponding author. Department of Orthodontics, Peking University School and Hospital of Stomatology, 22 Zhongguancun South Avenue, Haidian District, Beijing, China.

E-mail addresses: gulibaha_1972@163.com (G. Maimaitili), chenfeng2011@hsc.pku.edu.cn (F. Chen), jxlin@pku.edu.cn (J. Lin).

Peer review under responsibility of Chongqing Medical University.

¹ Contributed equally to this work.

² Present address: Key Laboratory of Shaanxi Province for Craniofacial Precision Medicine Research; Department of Orthodontics, College of Stomatology, Xi'an Jiaotong University, Xi'an 710004, China.

analysis;
PTCH1;
 Whole-exome
 sequencing

mutation. Structural modeling revealed a truncation starting from the middle of the second extracellular domain of *PTCH1* protein. This may damage its ligand recognition and sterol transportation abilities, thereby affecting the Hh signaling pathway. Biochemical assays indicated that the R945X protein had reduced stability compared to the wild-type *in vitro*. In addition, we reviewed the locations and mutation types of *PTCH1* variants in individuals with clefting phenotypes, and analyzed the associations between clefts and locations or types of variants within *PTCH1*. Our findings provide further evidence that *PTCH1* variants result in orofacial clefts, and contributed to genetic counseling and clinical surveillance in this family. Copyright © 2020, Chongqing Medical University. Production and hosting by Elsevier B.V. This is an open access article under the CC BY-NC-ND license (<http://creativecommons.org/licenses/by-nc-nd/4.0/>).

Introduction

Human Patched 1 (*PTCH1*) is identified as a tumor suppressor gene that encodes a membrane-embedded receptor of approximately 140 kDa. It plays a pivotal role in the Hedgehog (Hh) signaling pathway, which governs embryogenesis and postnatal tumorigenesis.^{1–3} When the secreted Hh signals are absent, *PTCH1* inhibits Smoothed (SMO),^{4,5} another membrane protein, and represses the signaling pathway. Activation of Hh signaling is initiated by recognition and binding of Hh and *PTCH1*, which relieves the inhibition of SMO, and regulates downstream transcriptional events.² Compromised or unrestrained Hh signaling may lead to birth defects or tumorigenesis.

The full-length *PTCH1* protein consists of 1447 amino acids. It comprises two extracellular domains (ECDs), 12 transmembrane segments (TMs) and a large intracellular loop. And the TMs 2–6 of *PTCH1* form the sterol-sensing domain (SSD).⁶

PTCH1 has been proven as a gene responsible for nevoid basal cell carcinoma syndrome (NBCCS), previously termed as Gorlin syndrome,⁷ which is characterized by various developmental anomalies and predisposition to form a variety of tumors. To date, more than 400 disease-associated *PTCH1* variants in NBCCS individuals have been reported.⁸ There is also evidence that *PTCH1* is involved in the etiology of orofacial clefting. A genome-wide association study (GWAS) based on a large Chinese cohort identified an intronic SNP located in the *PTCH1* gene that is associated with non-syndromic cleft lip with or without palate (NSCL/P).⁹ Next-generation sequencing found a *PTCH1* variant that was potentially causative for non-syndromic CL/P in a pedigree.¹⁰ Craniofacial abnormalities have been identified in *Ptch1*-defective mice, including cleft lip and clefting of the secondary palate.^{11,12} Notably, CL/P has actually been observed in NBCCS individuals, but with a low prevalence of 4%–9%.^{13,14} It remains unclear whether the locations and types of variants within *PTCH1* are related to different clinical manifestation.

Here, we identified a rare *PTCH1* variant through whole-exome sequencing (WES) for a family presenting with orofacial clefts. One of the family member did not show overt clefts but had subclinical phenotypes. The patients were diagnosed with suspected NBCCS. *In-silico* and *in-vitro* studies were performed to examine the pathogenicity of the variant. Furthermore, all *PTCH1* variants reported in

individuals with CL/P phenotypes were reviewed, and an up-to-date genotype-phenotype correlation will be discussed.

Materials and methods

Study subjects

We recruited a Chinese family with orofacial cleft as major manifestation, with the approval of the Human Research Ethics Committee of Peking University Hospital of Stomatology (PKUSSIRB-20150012). All participants underwent comprehensive history taking and physical examination. A panel of 64 unrelated and unaffected subjects also participated in the study. Informed consent was obtained from all the individual included in the study.

DNA extraction and WES

Genomic DNA of each participant was isolated from peripheral blood sample with the QIAamp DNA Blood Mini Kit (QIAGEN, Redwood City, CA, USA). High-throughput sequencing of the DNA libraries enriched with exonic sequences was performed. Sequencing files were generated using the BGISEQ-500 platform (BGI Inc., China) and mapped to the hg19 reference genome.

Variants screening strategy

Consecutive screening steps were applied. First, we included the variants with minor allele frequency (MAF) < 0.005 in 1000 Genomes Project Asian Database and that were protein-altering (nonsynonymous, missense, splicing, frameshift, etc.). Considering that the maternal grandmother of the proband did not show overt clefts but high-arched palate and occult uvula fissure, subsequent analyses were conducted respectively under the assumptions that she was (1) unaffected or (2) affected with subclinical phenotypes. Variants compatible with dominant or recessive models were filtered accordingly. Bioinformatic tools were used to predict any potentially damaging effects of the variants, including SIFT, PolyPhen2, LRT, MutationAssessor, RadialSVM, MutationTaster, LR and FATHMM.

After that, we performed web crawler combining literature review to help identify the most possible causative

variant. Briefly, we used in-house script to search all the gene symbols of the variants in the Pubmed Database, using the keywords [(specific gene symbol[Title/Abstract]) AND (cleft lip[Title/Abstract]) OR cleft palate[Title/Abstract]) OR orofacial cleft[Title/Abstract]) OR craniofacial defect [Title/Abstract]]. The web crawler process would output the number of literatures that mentioned both the specific gene and CL/P, so we could gain a quick perspective on the association between genes and CL/P. After that, we searched manually using the same keywords, to purposefully assess the reported evidence between genes and orofacial clefts, and to identify the candidate variant.

Sanger sequencing validation

We performed Sanger sequencing to analyze the candidate alleles genotype for the five family members. We also screened the 64 controls to determine the frequency of the variant, using the PCR primers: forward (5'-GGGGTTGTATCCCATTA-3') and reverse (5'-CAGTAGG-CATTCTATTCTTTG-3'); expected amplicon size 484 bp. PCR cycling condition consisted of 94 °C for 30 s, 54 °C for 30 s, 72 °C for 45 s with 35 cycles, and a final extension at 72 °C for 10 min. We analyzed the sequencing data using Chromas software.

Three-dimensional mimic modeling analysis of PTCH1 variant

The cryo-EM structure of human PTCH1 protein (PDB code: 6DMB)⁹ was used as a template. Three-dimensional modeling of PTCH1 variant was carried out by SWISS-MODEL (<https://www.swissmodel.expasy.org/>). All structure figures were prepared using PyMol.¹⁵

Plasmid construction, cell culture, and transfection

Full-length *PTCH1* gene sequence was a gift from Dr. Tiejun Li¹⁶ and was cloned into pcDNA3.1 vector with an N-terminal FLAG tag, named FLAG-PTCH1 WT. The *PTCH1* mutant was generated using the Fast Site-Directed Mutagenesis Kit (TIANGEN, China), named FLAG-PTCH1 R945X. The constructs were verified through Sanger sequencing.

The HEK-293FT cells were grown in 10 cm plates in Dulbecco's Modified Eagle's Medium (DMEM; Gibco, Waltham, MA, USA) supplemented with 10% FBS and 1% penicillin/streptomycin. After exceeding 70% confluence, the cells were transiently transfected with the expression plasmids using Lipofectamine 3000 Reagent (Invitrogen, Waltham, MA, USA) according to the manufacturer's instructions.

Plasma membrane protein isolation, immunoprecipitation (IP), and Western blotting

The cells were harvested 48–56 h after transfection. Plasma membrane protein was conducted using Minute Plasma Membrane Protein Isolation and Cell Fractionation Kit (Invent Biotechnologies, Plymouth, MN, USA). All procedures were performed on ice and followed

manufacturer's recommended protocols. The BCA Protein Assay Kit (CW BIO, China) was used to measure the protein concentration of each sample.

Subsequently, equivalent protein samples (about 200 µg each) were diluted with NP-40 buffer. We incubated them with 2 µL of anti-FLAG rabbit monoclonal antibody (CST, Danvers, MA, USA), followed by incubation with 40 µL of Protein A Magnetic Beads (Thermo Scientific, Waltham, MA, USA) at room temperature for 1 h. The immune complexes were washed three times at room temperature.

The plasma membrane samples, IP products and remnants were separated by 10% SDS-PAGE and transfected to 0.45 mm PVDF membrane. Membranes were incubated with mouse monoclonal anti-FLAG antibody (1:1000; CST, USA). A monoclonal anti- α 1-Na-K ATPase antibody (1:1000; Abcam, Cambridge, MA, USA) was used as membrane protein loading control, followed by fluorescent secondary antibodies. We used the Odyssey LI-COR Imaging System (LI-COR Corporate, Lincoln, NE, USA) to visualize the samples. Western blotting data were analyzed with Image J software with Student's *t*-test; *P* < 0.05 was statistically significant.

Literature review and genotype-phenotype correlation analysis

To explore the distribution and mutation type of *PTCH1* mutations in individuals with CL/P phenotypes, all *PTCH1* mutations reported in Human Gene Mutation Database (HGMD) public version and a *PTCH1* gene locus-specific database using the Leiden Open Variation Database (LOVD)⁸ were extracted for review in July 2019. Additional literature search from January 2016 to August 2019 was conducted using PubMed. The keywords used were "PTCH1" (or its synonyms) and "variant or mutation" (or their synonyms). All associated articles were downloaded. Studies were included when *PTCH1* variants with definite variant information were reported in patients with clefts phenotypes. Nucleotide and amino acid numbering were based on NCBI reference sequence NM_000264.3 and NP_000255.2.

Results

Clinical manifestations

A three-generation pedigree was recruited, as shown in Fig. 1A. The 8-year-old male proband (III-1) showed bilateral complete cleft lip and palate, and had received repair surgeries (Fig. 1B). His mother (II-2) had left cleft lip and ipsilateral alveolar bone cleft, with severity milder than III-1 (Fig. 1C). The maternal grandmother (I-2) did not show overt cleft phenotype by appearance. Intraoral examination showed multiple root remnants due to caries, and she wore a removable partial denture to restore occlusal function. The palatal area was not fully presented due to sheltering by the denture. The grandmother was initially classified as unaffected for variant screening, and no variant was found. However, a high-arched palate was noted on re-examination without the denture. An occult fissure on the uvula was found (Fig. 1D). Therefore,

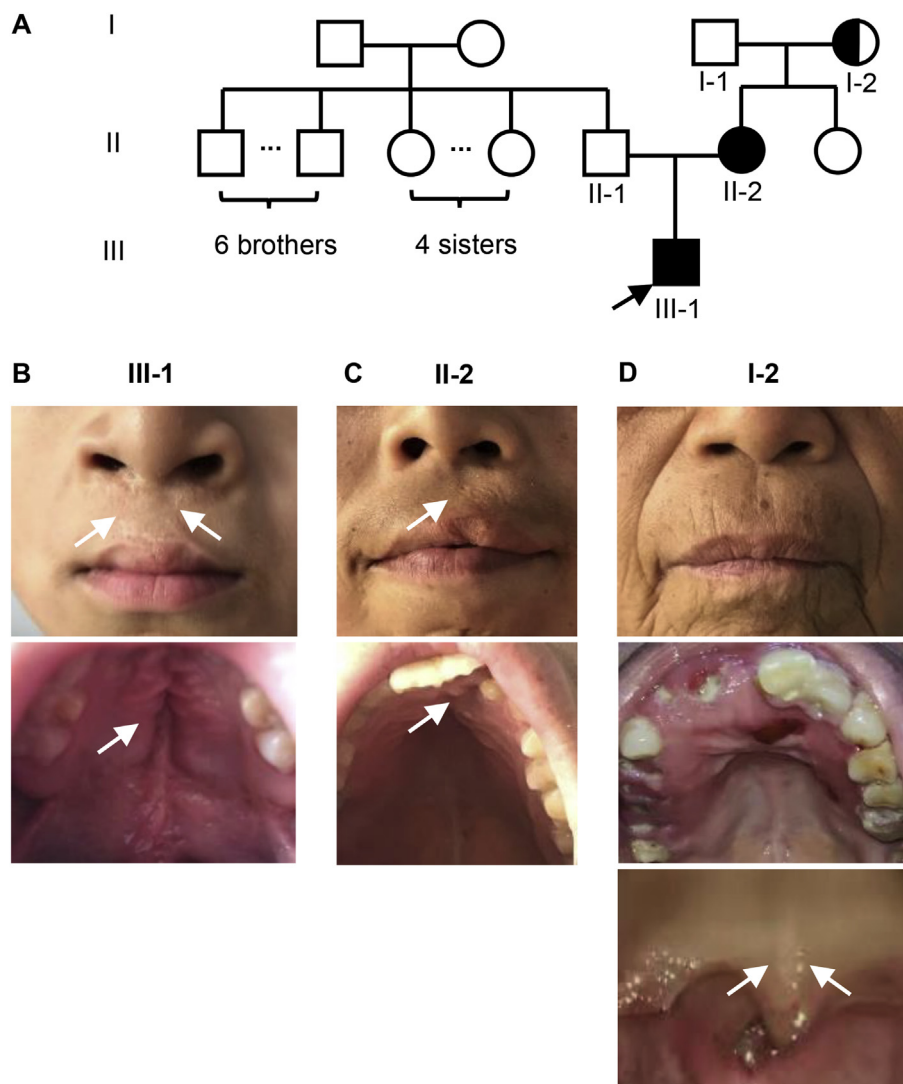


Figure 1 Pedigree and phenotypes of family members. (A) The filled and unfilled symbols indicate affected and unaffected subjects, respectively. The half-filled circle indicates that I-2 has subclinical phenotypes. Arrow indicates the proband. (B-D) Lip and palate phenotypes of III-1, II-2 and I-2.

she was classified as an affected family member with subclinical phenotypes. History collection and general examination were conducted. All three individuals had strabismus. No basal cell carcinomas or palmer/plantar pits were found, and there were no other general symptoms. The family members denied a history of keratocystic odontogenic tumors (KCOTs). The proband's father (II-1) and maternal grandfather (I-1) were clinically unaffected.

WES and variant screening identified a rare *PTCH1* variant

To localize the causative variant, we conducted WES on the five family members. On average, each sample obtained 25.04 Gb mappable exome sequencing data. In addition, they yielded a mean sequencing depth >265-fold. Within the exonic regions, 99.57% were covered at least four-fold

(Table S1). After mapping the sequences, we obtained 120654 variants on average (Table S2). The qualified sequencing data were used for further analysis.

A consecutive screening strategy was applied (Fig. 2), first based on variant frequency and functional alterations in coding regions, and 1739 variants remained on average. Inheritance pattern filtering was then performed. The member I-2 was initially regarded as an unaffected individual, as mentioned above, and both recessive (one variant left) and dominant/*de novo* (16 variants left) were considered. However, none of the variants was predicted to be deleterious or reported to be associated with CL/P.

On re-examination, I-2 was confirmed to be affected with subclinical phenotypes. Therefore, the possible inheritance pattern could be dominant (120 variants left) or recessive (null). Finally, a nonsense variant in the *PTCH1* gene (NM_000264.3 c.2833C > T p.R945X) was suggested to be potentially pathogenic.

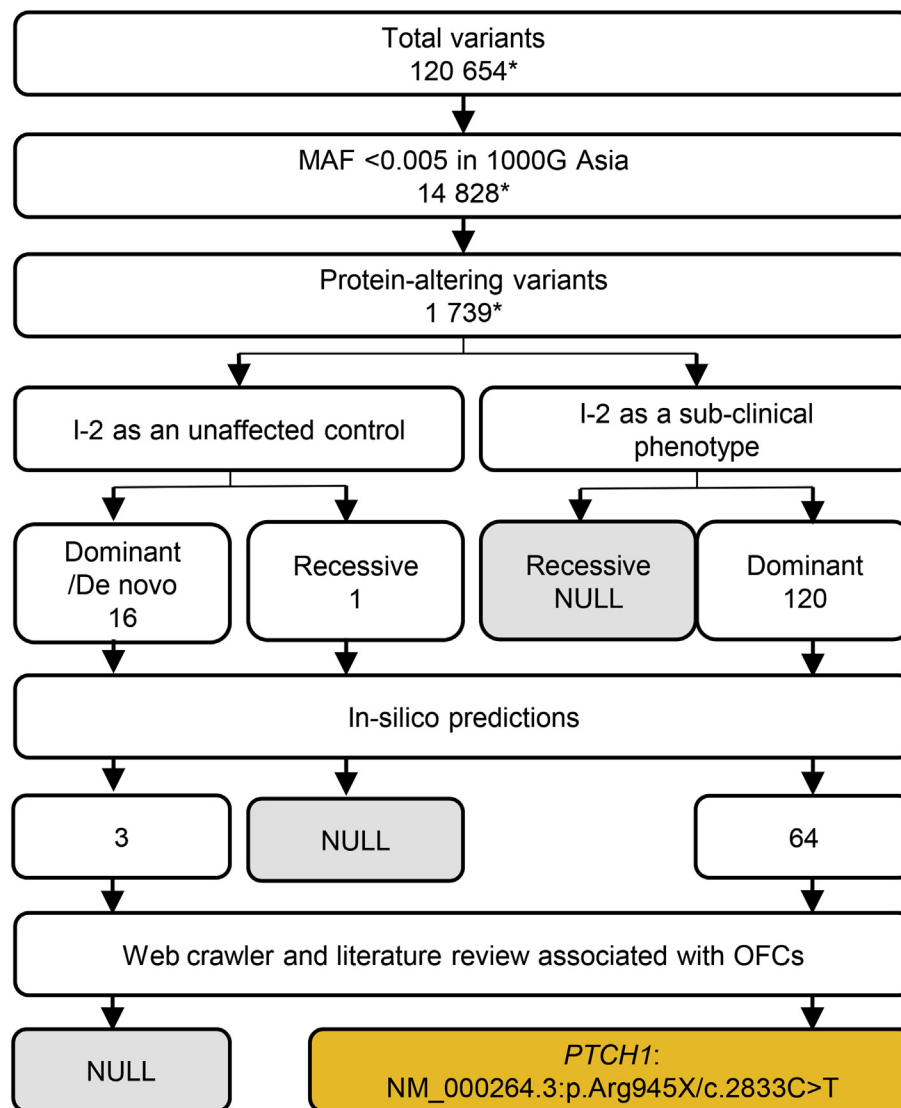


Figure 2 Variant screening flowchart. Numbers marked with * indicate the mean values of the remaining variants in each subject.

Sanger sequencing validated the *PTCH1* variant

The suspected variant was validated by Sanger sequencing, and found to be heterogeneous in the three affected members (III-1, II-2 and I-2). The unaffected individuals (II-1 and I-1) had the wild-type genotype, which was consistent with the results of WES and the autosomal dominant inheritance pattern (Fig. 3A). The variant was also not detected in our cohort of unrelated unaffected subjects.

Three-dimensional modeling indicated probable damaging effects

The c.2833C > T variant resulted in truncation in the middle of the second extracellular domain (ECD2) of the PTCH1 protein (Fig. 3B). The predicted three-dimensional structure for this R945X protein differed significantly from that of the wild-type protein. The last five transmembrane domains (TMs 8–12) were missing in the mutant (Fig. 3C).

However, the structure of the large intracellular domain, which is located at the N-terminus of the truncated site, was also predicted to be markedly altered. Focusing on the extracellular portion (Fig. 3D), differences were found mainly in the C-terminus. A loop-like structure, a few β -sheets, and some α -helices were missing, altering the normal structure and function of the extracellular domains in the mutant protein.

Immunoprecipitation implied decreased stability of PTCH1 R945X

To elucidate the pathogenicity of the R945X variant, we performed biochemical experiments to determine whether the protein function was affected. Two plasmids (FLAG-PTCH1 WT and R945X) were transfected into HEK-293FT cells, followed by plasma membrane protein extraction and Western blotting. No significant differences in protein expression between wild-type PTCH1 and the R945 mutant

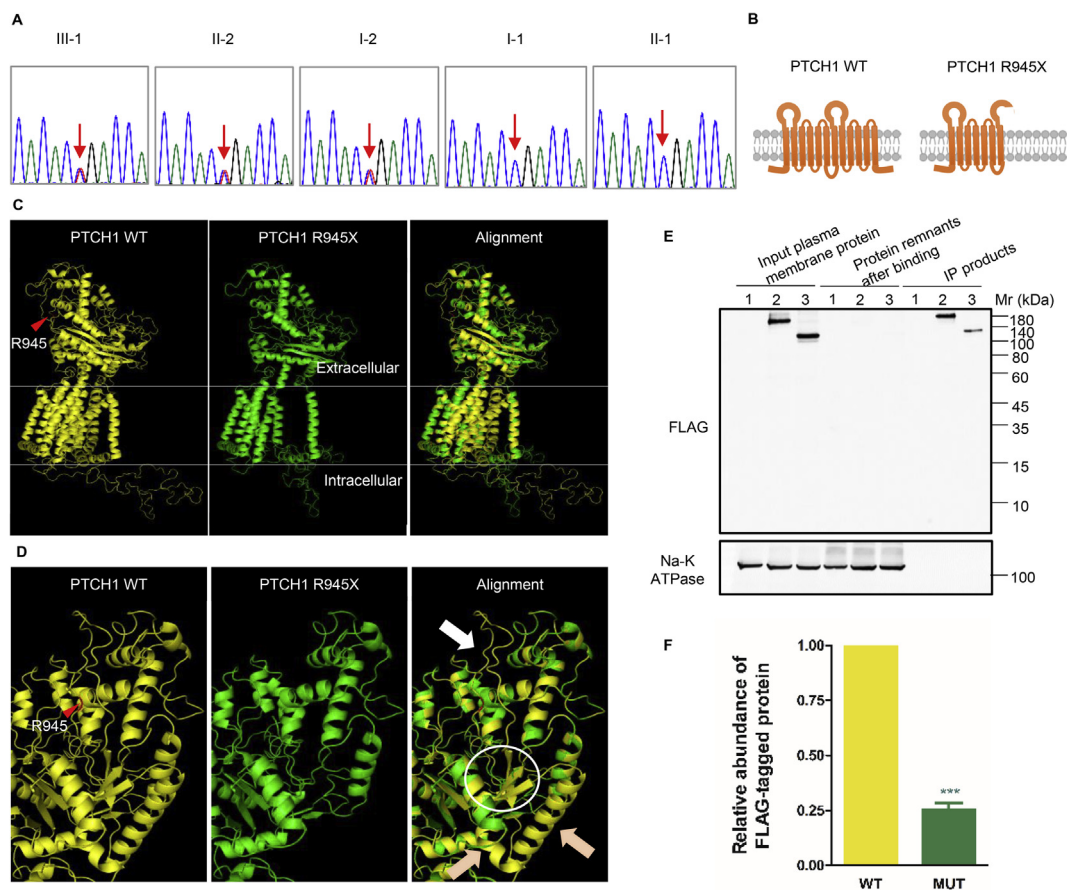


Figure 3 Sanger confirmation, *in-silico* and *in-vitro* studies of the mutant. **(A)** Sanger sequencing chromatograms of the family members. Red arrows indicate the mutant site. **(B)** Sketch diagram of PTCH1 wild-type (WT) and mutant (R945X) protein. **(C)** Overall view of homology models for WT (yellow) and R945X (green) protein. Red arrowhead indicates the mutant site. **(D)** Magnified and angle-adjusted view of extracellular domains. In the R945X protein, a loop-like structure (white arrow), three β -sheets and two α -helices (pink arrows) are missing. **(E-F)** Immunoprecipitation of FLAG-tagged PTCH1 WT and PTCH1 R945X proteins indicated a decreased stability of mutant protein. The normalized values represent mean (SD). *** $P < 0.001$.

(Fig. 3E). We then performed immunoprecipitation assay and immunoblotting analyses. In comparison with the wild-type protein, the R945X mutant showed approximately 75% lower relative abundance on immunoprecipitation assay ($P < 0.001$) (Fig. 3E and F), which implied a decrease in the stability of the R945X mutant *in vitro*.

Mutation types and distribution pattern of *PTCH1* variants in individuals with CL/P phenotypes

Including the c.2833C > T p.R945X variant in the present study, in total 25 *PTCH1* variants have been identified in subjects affected with CL/P (Fig. 4A; Table S3). Missense variants were mostly found to be associated with CL/P (40%) (Fig. 4B). Frameshift (24%) and nonsense (20%) variants, both causing truncation, were also major causes of CL/P phenotypes. No large deletions or duplications were found.

The variants were predominantly found in the two ECDs (64%) (Fig. 4C), and 22% of the variants were located in the TMs, among which two variants were detected in the sterol-sensing domain.

Discussion

In this study, we identified a rare *PTCH1* variant (c.2833C > T p.R945X) by WES in a Chinese family mainly with orofacial clefts and subclinical phenotype. We conducted molecular structural modeling and biochemical assays to study the pathogenicity of the mutation.

In our previous work involving identification of the genetic mutations underlying CL/P,^{10,17,18} many variants were left after the traditional screening process, and a manual literature search was required to identify the candidate(s). In this study, we employed a web crawler strategy for the first time to narrow down the list of variants. This method may contribute to future studies regarding CL/P and other human disorders.

When identifying *PTCH1* c.2833C > T p.R945X in the CL/P-affected family in this study, we found that the same germline variant had been reported in an individual with NBCCS,¹⁹ in spite of different position numbering due to dissimilar reference sequences.^{7,20} The NBCCS individual, however, was not reported to have cleft phenotype, which would have been difficult to overlook if it had been present. Whereas in this study, three members of the family

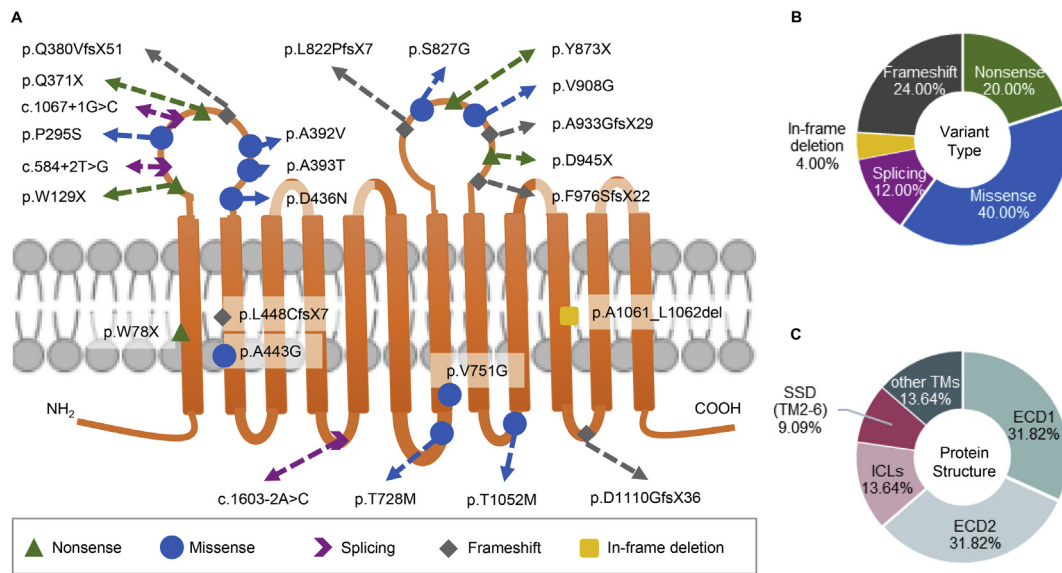


Figure 4 Mutation type and distribution of reported CL/P-causing *PTCH1* variants. **(A)** Sketch diagram of the 25 variants. Variants are described in amino-acid alteration form except for the splicing variants. For the latter, they are labeled on the figure based on the introns they are located at. **(B)** Pie chart for mutation type ($n = 25$). **(C)** Pie chart for protein localization distribution ($n = 22$). Splicing variants are not calculated because of unknown protein alterations.

showed overt orofacial clefts except the maternal grandmother, who had subclinical phenotypes of high-arched palate and submucous cleft palate.

It is of interest that individuals carrying the identical variant somehow display highly variable phenotypic expressivity and penetrance. These phenomena implied that attention should be paid to subclinical phenotypic features in individuals with CL/P and their “unaffected” relatives.²¹ Subclinical phenotyping holds great promise to enhance the search for causative genetic variants, such as orbicularis oris defects^{22,23} and submucous cleft palate as detected in this study, and to contribute to clinical risk assessment.

Second, variable penetrance poses a key challenge for understanding how genetic variants act in human diseases. This may be related to other variants with regulatory elements outside coding regions of genes.²⁴ A recent genome-wide study based on diverse population datasets provided evidence that common cis-regulatory variants modify the penetrance of rare pathogenic coding variants and affect disease risk depending on the haplotype combination.²⁵ This highlighted the importance of taking regulatory elements into consideration along with rare coding variants in future studies. Whole-genome sequencing would allow tracking of these variants as they usually regulate genes across substantial genomic distances.

Further phenotyping of the members of the family included in this study is challenging as they reside in a remote area. However, considering the recorded phenotypes (CL/P and strabismus) and the same variant as the previously reported NBCCS patient, we suspect that they are affected by NBCCS. We will strive to obtain complete information, and perform clinical surveillance and future genetic counseling for this family as they are probably at high risk of NBCCS.

The functional changes in the *PTCH1* R945 variant can be explained by its structural alterations as indicated by

three-dimensional modeling. The two extracellular domains, ECD1 and ECD2, of wild-type *PTCH1* together serve as the binding site for Hh ligands.²⁶ The recognition is completed through extensive polar interactions, and glutamic/aspartic acid residues distributed at residues 947–958 in ECD2 form the interface.⁶ Meanwhile, a hydrophobic conduit was observed to course through the extracellular domains with cholesterol transporter-like function.^{27,28} Upon binding with Hh, sterol is transported into the inner side of the plasma membrane and binds to the transmembrane domains of SMO, which drives the activation of SMO.⁵ The truncated mutant, however, has disruption of not only the Hh binding site, but also the cholesterol transport tunnel, influencing the normal activation of the Hh signaling pathway during embryogenesis. Another significant structural change was observed in the intracellular domain, which has been reported to regulate the subcellular localization of M-phase promoting factor.²⁹ Thus, the mutation may affect cell proliferation. The consequences of the deficiency of the C-terminal transmembrane domains (TMs 8–12) remain unclear, but it probably affects the stability, as *in vitro* studies indicated decreased stability of the mutant protein in this study.

No clear evidence has been provided on whether the types and locations of mutations within *PTCH1* are relevant to clinical manifestation in NBCCS. However, mutation type pattern diversity among different clinical symptoms could be found. In this study, among *PTCH1* variants carried by individuals with CL/P, truncation- and non-truncation-causing variants were found equal in quantity (both 44%). No large deletions and duplications that encompassed more extensive structural changes were found in CL/P-affected individuals. In contrast, in patients with NBCCS-associated KCOTs, merely 27% variants were non-truncation causing, and over 60% *PTCH1*

variants resulted in truncation of the protein.³⁰ The distribution pattern revealed the two extracellular domains as variation hotspots.

In conclusion, a rare *PTCH1* nonsense variant was characterized in a family suffering from CL/P with variable penetrance and suspected to be affected by NBCCS. We speculated on the pathology based on the results of bioinformatics and biochemical assays, yet further cellular and molecular studies are needed. A crucial finding in this study was the identification of subclinical phenotypes. The phenomenon of individuals carrying the same coding variants but showing inconsistent phenotypes indicates the importance of exploring joint functional effects of regulatory and coding variants. Genome-wide sequencing data and analyses would provide approaches to clarifying the underlying etiology. Finally, the findings presented here contributed to genetic counseling and clinical management for this family.

Conflict of Interests

The authors declare no conflict of interests.

Acknowledgements

This study was supported by the National Natural Science Foundation of China (grant numbers: 81870747, 81860194, and 31771619) and Beijing Municipal Natural Science Foundation (grant number: 7182184). We appreciate the involvement of all the participants. We also thank Professor Tiejun Li for his kindly gift.

Appendix A. Supplementary data

Supplementary data to this article can be found online at <https://doi.org/10.1016/j.gendis.2019.12.010>.

References

- Ingham PW, Nakano Y, Seger C. Mechanisms and functions of Hedgehog signalling across the metazoa. *Nat Rev Genet.* 2011; 12(6):393–406.
- Briscoe J, Therond PP. The mechanisms of Hedgehog signalling and its roles in development and disease. *Nat Rev Mol Cell Biol.* 2013;14(7):416–429.
- Pak E, Segal RA. Hedgehog signal transduction: key players, oncogenic drivers, and cancer therapy. *Dev Cell.* 2016;38(4): 333–344.
- Martín V, Carrillo G, Torroja C, Guerrero I. The sterol-sensing domain of Patched protein seems to control Smoothed activity through Patched vesicular trafficking. *Curr Biol.* 2001; 11(8):601–607.
- Deshpande I, Liang J, Hedeon D, et al. Smoothed stimulation by membrane sterols drives Hedgehog pathway activity. *Nature.* 2019;571(7764):284–288.
- Gong X, Qian H, Cao P, et al. Structural basis for the recognition of sonic hedgehog by human Patched1. *Science.* 2018; 361(6402),eas8935.
- Johnson RL, Rothman AL, Xie J, et al. Human homolog of patched, a candidate gene for the basal cell nevus syndrome. *Science.* 1996;272(5268):1668–1671.
- Reinders MA-O, van Hout AF, Cosgun B, et al. New mutations and an updated database for the patched-1 (*PTCH1*) gene. *Mol Genet Genomic Med.* 2018;6(3):409–415.
- Yu Y, Zuo X, He M, et al. Genome-wide analyses of non-syndromic cleft lip with palate identify 14 novel loci and genetic heterogeneity. *Nat Commun.* 2017;8,e14364.
- Zhao H, Zhong W, Leng C, et al. A novel *PTCH1* mutation underlies nonsyndromic cleft lip and/or palate in a Han Chinese family. *Oral Dis.* 2018;24(7):1318–1325.
- Feng W, Choi I, Clouthier DE, Niswander L, Williams T. The *Ptch1(DL)* mouse: a new model to study lambdoid craniosynostosis and basal cell nevus syndrome-associated skeletal defects. *Genesis.* 2013;51(10):677–689.
- Kurosaka H, Iulianella A, Williams T, Trainor PA. Disrupting hedgehog and WNT signaling interactions promotes cleft lip pathogenesis. *J Clin Investig.* 2014;124(4): 1660–1671.
- Fujii K, Miyashita T. Gorlin syndrome (nevoid basal cell carcinoma syndrome): update and literature review. *Pediatr Int.* 2014;56(5):667–674.
- Kimonis VE, Singh KE, Zhong R, Pastakia B, Digiovanna JJ, Bale SJ. Clinical and radiological features in young individuals with nevoid basal cell carcinoma syndrome. *Genet Med.* 2013;15(1): 79–83.
- Bramucci E, Paiardini A, Bossa F, Pascarella S. PyMod: sequence similarity searches, multiple sequence-structure alignments, and homology modeling within PyMOL. *BMC Bioinformatics.* 2012;13(Suppl 4),S2.
- Yu FY, Hong YY, Qu JF, Chen F, Li TJ. The large intracellular loop of *ptch1* mediates the non-canonical Hedgehog pathway through cyclin B1 in nevoid basal cell carcinoma syndrome. *Int J Mol Med.* 2014;34(2):507–512.
- Zhao H, Zhang M, Zhong W, et al. A novel *IRF6* mutation causing non-syndromic cleft lip with or without cleft palate in a pedigree. *Mutagenesis.* 2018;33(3):195–202.
- Meng P, Zhao H, Huang W, et al. Three *GLI2* mutations combined potentially underlie non-syndromic cleft lip with or without cleft palate in a Chinese pedigree. *Mol Genet Genomic Med.* 2019,e714.
- Hasenpusch-Theil K, Bataille V, Laehdetie J, Obermayr F, Sampson JR, Frischauf AM. Gorlin syndrome: identification of 4 novel germ-line mutations of the human patched (*PTCH*) gene. *Hum Mutat.* 1998;11(6),e480.
- Hahn H, Christiansen J, Wicking C, et al. A mammalian patched homolog is expressed in target tissues of sonic hedgehog and maps to a region associated with developmental abnormalities. *J Biol Chem.* 1996;271(21): 12125–12128.
- Dixon MJ, Marazita ML, Beaty TH, Murray JC. Cleft lip and palate: understanding genetic and environmental influences. *Nat Rev Genet.* 2011;12(3):167–178.
- Neiswanger K, Weinberg SM, Rogers CR, et al. Orbicularis oris muscle defects as an expanded phenotypic feature in non-syndromic cleft lip with or without cleft palate. *Am J Med Genet.* 2007;143A(11):1143–1149.
- Marazita ML. Subclinical features in non-syndromic cleft lip with or without cleft palate (CL/P): review of the evidence that subepithelial orbicularis oris muscle defects are part of an expanded phenotype for CL/P. *Orthod Craniofac Res.* 2007; 10(2):82–87.
- Cooper DN, Krawczak M, Polychronakos C, Tyler-Smith C, Kehrer-Sawatzki H. Where genotype is not predictive of phenotype: towards an understanding of the molecular basis of

- reduced penetrance in human inherited disease. *Hum Genet.* 2013;132(10):1077–1130.
25. Castel SE, Cervera A, Mohammadi P, et al. Modified penetrance of coding variants by cis-regulatory variation contributes to disease risk. *Nat Genet.* 2018;50(9):1327–1334.
 26. Marigo V, Davey RA, Zuo Y, Cunningham JM, Tabin CJ. Biochemical evidence that patched is the Hedgehog receptor. *Nature.* 1996;384(6605):176–179.
 27. Zhang Y, Bulkley DP, Xin Y, et al. Structural basis for cholesterol transport-like activity of the hedgehog receptor patched. *Cell.* 2018;175(5):1352–1364.
 28. Qi X, Schmiede P, Coutavas E, Li X. Two Patched molecules engage distinct sites on Hedgehog yielding a signaling-competent complex. *Science.* 2018;362(6410),eaas8843.
 29. Barnes EA, Kong M, Ollendorff V, Donoghue DJ. Patched1 interacts with cyclin B1 to regulate cell cycle progression. *EMBO J.* 2001;20(9):2214–2223.
 30. Guo YY, Zhang JY, Li XF, Luo HY, Chen F, Li TJ. PTCH1 gene mutations in Keratocystic odontogenic tumors: a study of 43 Chinese patients and a systematic review. *PLoS One.* 2013; 8(10),e77305.